VCD spectroscopic and molecular dynamics analysis of the Trp-cage miniprotein TC5b

ARTICLE *in* BIOPOLYMERS · JANUARY 2007

Impact Factor: 2.39 · DOI: 10.1002/bip.20709 · Source: PubMed

3 AUTHORS, INCLUDING:

Jeffrey Copps
The Scripps Research Institute
13 PUBLICATIONS **51** CITATIONS
SEE PROFILE

Sandor Lovas
Creighton University
123 PUBLICATIONS **2,059** CITATIONS
SEE PROFILE

VCD Spectroscopic and Molecular Dynamics Analysis of the Trp-Cage Miniprotein TC5b

Jeffrey Copps, Richard F. Murphy, Sándor Lovas
Department of Biomedical Sciences, Creighton University Medical Center, 2500 California Plaza, Omaha, NE

Received 17 October 2006; revised 12 February 2007; accepted 15 February 2007
Published online 26 February 2007 in Wiley InterScience (www.interscience.wiley.com). DOI 10.1002/bip.20709

ABSTRACT:

TC5b is a 20 residue polypeptide notable for its compact tertiary structure, a rarity for a short peptide. This structure is due to the "Trp-cage" motif, an association of aromatic, Pro, and Gly residues. The structure of TC5b has been fully characterized by NMR and electronic circular dichroism (ECD) studies, but has never been studied with vibrational circular dichroism (VCD) spectroscopy, which may reveal finer structure. In this study, we examine the VCD spectra of TC5b to characterize the spectroscopic signature of the peptide and its comprising structural elements. TC5b exhibited a negative-positive-negative triplet which is associated with α-helical structure in deuterated solvents but also signs of a polyproline II (PPII) helix in the amide I' region. Detection of this element was complicated by the aforementioned triplet form, as well as by an upfrequency shift in PPII helical elements due to the use of the deuterated organic solvents DMSO-d_6 and TFE-d_1. Nevertheless, while ECD spectra showed only α-helical structure for TC5b, VCD spectroscopy revealed a more complex structure which was in agreement with NMR results. VCD spectroscopy also showed a rapid conformational change of the peptide at temperatures above 35°C in D_2O and in aqueous solvent with greater than 75% DMSO-d_6 content. Molecular dynamics (MD) simulations to investigate this latter effect of DMSO-d_6 on TC5b were conducted in DMSO and 50% (v/v) DMSO in H_2O. In DMSO unfolding of the peptide was rapid while in 50% (v/v) DMSO in H_2O the unfolding was more gradual. © *2007 Wiley Periodicals, Inc. Biopolymers (Pept Sci) 88: 427–437, 2007.*

Keywords: VCD; molecular dynamics; TC5b; conformation; polyproline II

Correspondence to: Sándor Lovas, Department of Biomedical Sciences, Creighton University School of Medicine, 2500 California Plaza, Omaha, NE 68178, USA; e-mail: slovas@creighton.edu
Contract grant sponsor: NIH-BRIN
Contract grant number: P20 RR016469
Contract grant sponsor: Carpenter Endowed Chair in Biochemistry, Creighton University

This article was originally published online as an accepted preprint. The "Published Online" date corresponds to the preprint version. You can request a copy of the preprint by emailing the Biopolymers editorial office at biopolymers@wiley.com

INTRODUCTION

The 20-residue "miniprotein" TC5b (Asn-Leu-Tyr-Ile-Gln-Trp-Leu-Lys-Asp-Gly-Gly-Pro-Ser-Ser-Gly-Arg-Pro-Pro-Pro-Ser) is the product of truncation and mutation of the gila monster saliva peptide exendin-4.[1] Its short sequence and compact structure, a result of its unique "Trp-cage" motif,[2] make it an ideal model for the study of folding in proteins. The Trp6 side chain is enclosed by and has CH-π interactions[3] with the methylene groups of the side chains of Pro12, Pro18, and Pro19, as well as the α-hydrogen of Gly11. In addition, the NH group of Gly11 forms a hydrogen bond with the backbone carbonyl group of Trp6, and the side chain ring of Tyr3 interacts with the indolyl ring of Trp6. Another hydrogen bond forms

between the Trp6 indole NH group and the backbone carbonyl group of Arg16. These interactions form the Trp-cage, stabilizing the tertiary structure of the miniprotein.[1]

TC5b has been a powerful model for research into protein folding. Extensive folding studies using Molecular Dynamics (MD) simulations have found that TC5b folds within 4.1 μs, far faster than does any complete protein known, including WW domains and 16 residue β-hairpin fragments.[4] These simulations revealed that this expedience is due to two state-folding of the peptide, in which an intermediate state containing a metastable salt bridge between Asp9 and Arg16 is formed, facilitating the correct packing of the two hydrophobic cores separated by the salt bridge. This structure then collapses, the two cores form the larger Trp-cage hydrophobic core, and the salt bridge reforms later to give greater stability to the final structure.[5] A more recent fluorescence study,[6] however, showed a more complicated, hierarchical folding. Another computational study demonstrated locally driven folding pathways of the Trp-cage structure through stepwise elongation of the peptide chain.[7] Implicit solvent model simulations of TC5b structure have also shown that packing of the Trp6 side chain is the rate limiting step in the folding and have demonstrated the effectiveness of MD as a predictor of structure.[8–11] However, such simulations may, as discussed by Zhou,[5] have serious deficiencies.

TC5b has also been the subject of some spectroscopic analysis. Electronic circular dichroism spectroscopy (ECD) has shown that the peptide appears to be α-helical in aqueous buffer at pH 7 with and without 30% TFE,[1] and that the insertion of six Ala residues near the N-terminus dramatically stabilizes the α-helix and thus the Trp-cage fold, of which it is a major component.[12] NMR spectroscopy, however, has shown the existence of a β-turn in the central region of the sequence and a polyproline II (PPII) helix associated with the C-terminal region which contains the proline triplet Pro17–19.[1,13] These structures are not visible using ECD spectroscopy.[1]

Vibrational circular dichroism (VCD) spectroscopy monitors circular dichroism in numerous vibrational transitions, rather than in the limited electronic transitions measured by ECD spectroscopy,[14,15] which limit the resolution of fine structure. Additionally, the transitions of any aromatic groups present will overlap with those of other groups, further obscuring structural data obtained by ECD.[14,16] VCD eliminates these problems by having numerous vibrational transitions, as well as separation of carbonyl stretching vibrations from aromatic stretching vibrations. These advantages do come at the expense of longer data collection, higher sample concentration, and restricted use of water as a solvent. Extremely valuable data, however, can be obtained.

In the present study, VCD spectroscopy was used to examine the conformation of H/D-exchanged (predeuterated) and non-predeuterated TC5b in aqueous and organic deuterated solvents to discern fine structure. The results led to the use of explicit solvent MD simulations to examine the structure of the peptide in DMSO and 50% (v/v) DMSO in H_2O. TC5b has previously been simulated in explicit H_2O models,[5,10,17] so H_2O is not considered here as a solvent.

RESULTS AND DISCUSSION

VCD Measurements of TC5b

Figure 1A shows the normalized VCD spectra of TC5b in 100% D_2O. Spectra in the amide I' region (1600–1700 cm^{-1}), where the stretching vibration of the backbone carbonyl groups with the backbone NH groups deuterated (ND) appears, show a negative-positive-negative "split couplet" or triplet form, which is associated with α-helical structure in deuterated solvents.[14] The amide II region at 1500–1600 cm^{-1}, where the bending vibration of NH groups coupled to the CN stretching vibration of the amide groups appears, is flat in both samples, indicating a lack of NH groups and thus, strong H-D exchange on backbone NH amide groups, supporting that deuteration has affected the secondary structure of the peptide. The amide II' region at 1400–1500 cm^{-1}, where the bending vibration of ND groups coupled to the CN stretching vibration of the amide groups appears, has a negative peak in both groups, indicating the presence of ND groups and once again, strong H-D exchange on backbone amide groups. The IR spectra mirror these positive and negative peaks, showing absorption at roughly the same wavenumbers as the positive and negative peaks (in this case, as shoulders) in the amide I' region, and at the negative peak in the amide II' region.

The normalized VCD spectra of TC5b in 15 m*M* Na_2HPO_4 in D_2O (Figure 1B) are very similar to those of TC5b in D_2O, albeit containing smaller second negative peaks in the amide I' region. The predeuterated and non-predeuterated samples both contain large negative bands in the amide II' region and flat amide II regions, once again indicating strong H-D exchange. The IR spectra correspond in activity to the VCD spectra, similar to the D_2O measurement, showing a large positive peak with a trailing shoulder in the amide I' region and a positive peak in the amide II' region.

The normalized VCD spectra of TC5b in 30% (v/v) TFE-d_1 in 15 m*M* Na_2HPO_4 in D_2O are shown in Figure 1C. The second negative peaks show shoulders in both the predeuterated and non-predeuterated samples near 1628 cm^{-1}, and are smaller overall than in Figures 1A and 1B. This is most

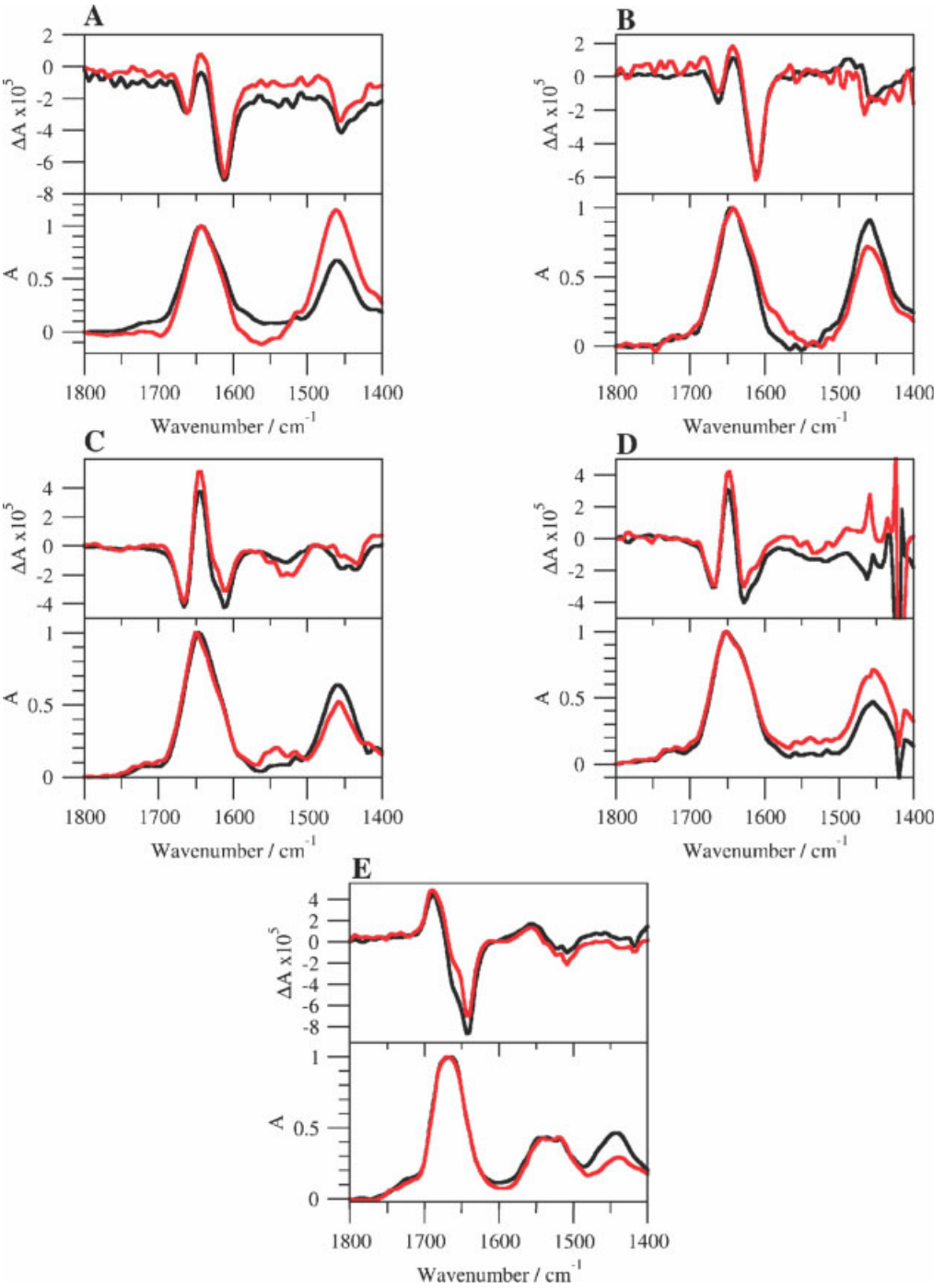

FIGURE 1 Normalized VCD spectra (top) and IR spectra (bottom) of TC5b in various solvents. Black, TC5b predeuterated; red, TC5b non-predeuterated. (A), D_2O; (B), 15 m*M* Na_2HPO_4 in D_2O; (C), 30% (v/v) TFE-d_1 in 15 m*M* Na_2HPO_4 in D_2O; (D), 5% (v/v) DMSO-d_6 in TFE-d_1; (E), DMSO-d_6.

likely due to the matrix-forming effect of TFE-d_1, excluding D_2O from access to the peptide backbone.[18,19] This is supported by the spectra of the amide II and II' regions which show some evidence for H-D amide exchange, but also some lack of exchange in both samples. The IR spectra once again mirror the VCD positive and negative peaks, though in this measurement, absorbances in the amide II region correspond to the lack of exchange of hydrogen for deuterium, unlike for the other measurements, where no lack of exchange and thus no activity in the amide II region occurred.

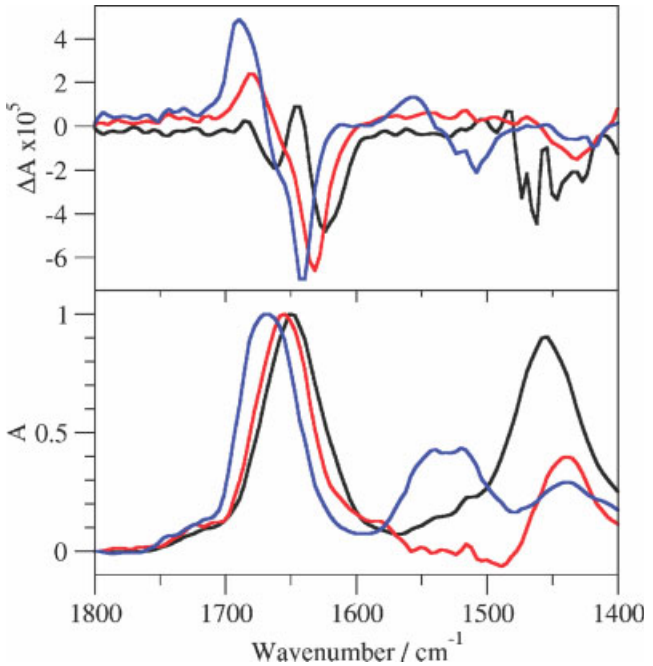

FIGURE 2 The effect of DMSO-d_6 content on the normalized VCD (top) and IR (bottom) spectra of TC5b in D_2O (v/v). Black, 50% (v/v) DMSO-d_6 in D_2O; red, 75% (v/v) DMSO-d_6 in D_2O; blue, 100% DMSO-d_6.

The normalized VCD spectra of TC5b in 5% (v/v) DMSO-d_6 in TFE-d_1 (Figure 1D) show shoulders on the second negative peaks, although they are on the opposite side of the minima near 1612 cm^{-1}. In addition, the minima of the negative peaks are at 1628 cm^{-1}, 16 wavenumbers upfrequency from the previous minima near 1612 cm^{-1}. The signal in the amide II' region is obscured by the absorbance of TFE-d_1, prohibiting the observation of evidence for H-D amide exchange, though the amide II region does shows some lack of exchange. The IR spectra absorptions correspond to the VCD positive and negative peaks as previously.

The normalized VCD spectra of TC5b in DMSO-d_6 (Figure 1E) show that TC5b loses its stable α-helical conformation and adopts a new conformation. The triplet signature is lost, and a new, negative couplet with a midpoint near 1670 cm^{-1} is formed. This is clearly not representative of an α-helix. In the IR spectra, corresponding positive and negative peaks are seen in all three regions, especially the amide II region, where large absorption had not previously been seen. Previously, synthetic exendin-4 was shown to have markedly lower chemical shift deviations in 98% (v/v) DMSO in H_2O than in 30% (v/v) TFE in H_2O, 60% (v/v) DMSO in H_2O, and 30% aqueous glycol.[20] A loss of α-helical structure in the exendin-4 analog TC5b is then likely in DMSO-d_6, but the conditions necessary to effect such a change, as well as the nature of the resulting structure, are not known. Therefore, to determine the amount of DMSO-d_6 necessary to effect this conformational change in the α-helical structure, a series of measurements of the TC5b VCD spectrum were taken in D_2O with an increasing concentration of DMSO-d_6. ECD spectroscopy cannot be used with DMSO. The spectra from this series of measurements are shown in Figure 2. In 50% (v/v) DMSO-d_6 in D_2O, the VCD spectra of TC5b in the amide I' region remains α-helical. This structure remains intact until the peptide is dissolved in 75% (v/v) DMSO-d_6 in D_2O, where an overall conformational change occurs, and the VCD spectra begins to resemble that of the spectra seen for the 100% DMSO-d_6 measurement: a negative couplet with a shoulder on the negative peak and a midpoint shifted upfrequency, in this case, to 1663 cm^{-1}. The IR spectra follow these changes, with the amide I' region positive peak staying at about 1650 cm^{-1} before shifting upfrequency as DMSO-d_6 content surpasses 75% of the total volume.

VCD measurements of TC5b structure in D_2O at increasing temperature were recorded to determine at what temperature the Trp-cage would unfold. The results (Figure 3) clearly show that, above 35°C, the α-helical structure of the peptide breaks down into a random meander structure as the deuterated triplet structure is lost in the amide I' region. The IR spectra show a positive peak and shoulders corresponding to the VCD features, as previously.

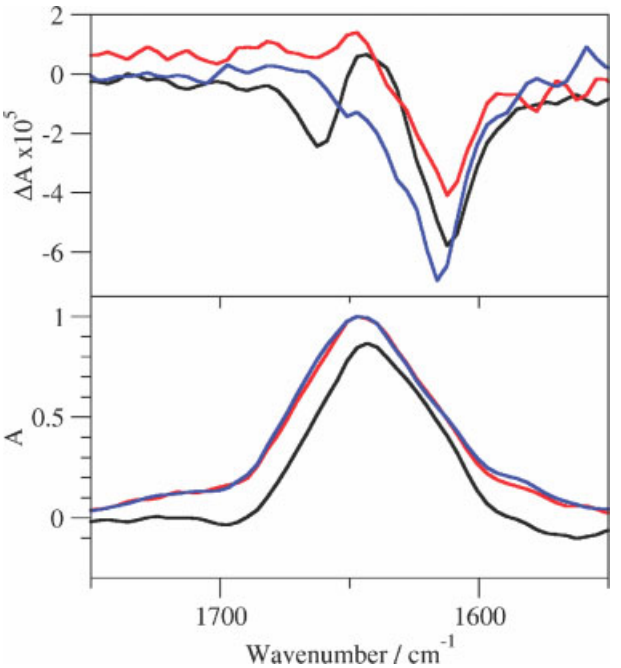

FIGURE 3 The effect of temperature on the normalized VCD (top) and IR (bottom) spectra of TC5b in D_2O in the amide I' region. Black, 5°C; red, 35°C; blue, 55°C.

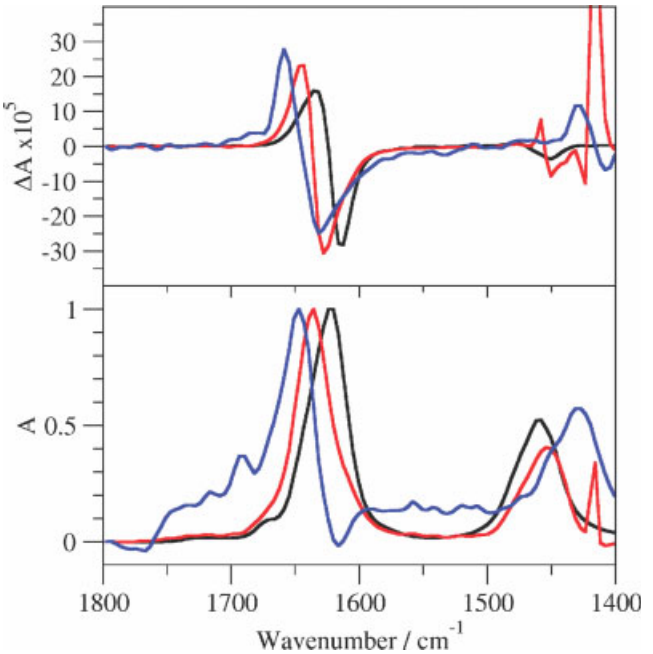

FIGURE 4 Normalized VCD (top) and IR (bottom) spectra of poly-L-Pro in various solvents. Black, D_2O; red, 5% (v/v) DMSO-d_6 in TFE-d_1; blue, DMSO-d_6.

Comparison With Poly-L-Pro

VCD spectra of both PPII helices and random meander conformations have a negative couplet,[21,22] although, the amide I region for PPII helices is shifted toward lower frequency by 23 cm^{-1}. The VCD spectra of poly-L-Pro (Figure 4) show that the characteristic negative couplet of the PPII helix of the amide I' region is upfrequency of its normal position near 1620 cm^{-1} when the peptide is exposed to organic solvents. The couplet midpoint, at 1624 cm^{-1} in D_2O, is at 1637 cm^{-1} in 5% (v/v) DMSO-d_6 in TFE-d_1, and at 1646 cm^{-1} in 100% DMSO-d_6, a change of 22 wavenumbers. The IR spectra peaks in the amide I' region shift correspondingly.

The minimum, 1612 cm^{-1}, of the second negative peaks of the normalized VCD spectra of TC5b in D_2O and in 15 m*M* Na_2HPO_4 in D_2O is identical to that of poly-L-Pro in D_2O (Figure 5A and 5B). However, when the shifted spectra of poly-L-Pro in 5% (v/v) DMSO-d_6 in TFE-d_1 is compared with the VCD spectra of TC5b in 5% (v/v) DMSO-d_6 in TFE-d_1 and in 30% (v/v) TFE-d_1 in 15 m*M* Na_2HPO_4 in D_2O (Figures 5C and 5D), the negative peak coincides with the shoulder in the latter spectra and the negative peak in the former, both at 1628 cm^{-1}. This is also seen in the respective IR spectra. Because of the clear correspondence of these features, it is concluded that they represent the PPII helical content of TC5b in TFE and H_2O. This content is masked by deuteration of the peptide backbone. The effect especially occludes the PPII signature in 15 m*M* Na_2HPO_4 in D_2O and in 100% D_2O, when H-D amide exchange is exceptionally high. However, the helix is revealed by the PPII shift in TFE-d_1 and DMSO-d_6, as well as by the restriction of access of deuterating agents to the peptide backbone by these solvents. The best example of this is the spectrum of TC5b in 5% (v/v) DMSO-d_6 in TFE-d_1 (Figure 5D). Here, the trailing shoulder near 1612 cm^{-1} is clearly the minimum of the negative peak of the α-helix triplet, its intensity reduced greatly by lack of deuteration because of the high TFE-d_1 content, even more so than in 30% (v/v) TFE-d_1 in 15 m*M* Na_2HPO_4 in D_2O (Figure 5C). The intensity of the PPII contribution in both spectra, however, remains strong.

MD Simulations

MD simulations were performed to further investigate the earlier finding of the unfolding of TC5b in increasing concentration of DMSO. DSSP analysis of the trajectory for TC5b in DMSO is shown in Figure 6A. The initial α-helical segment is broken down into *β*-turn and then to bend and random meander structure starting at 14 ns (losing one turn of the helix as early as 9 ns), and the *β*-turn structure of residues 10–12 is lost even earlier. Looking at inter-residue distances in the Trp-cage, the Trp6 residue is removed from proximity to Tyr3 and Gly11 (Figure 6B) near the breakdown of the α-helix. Trp6 is also moved far away from Pro12 and Pro18–19 at this time (Figure 6C). Additionally, Asp9 and Arg16 are moved apart quickly (Figure 6D). All these movements of key Trp-cage residues indicate the destabilization of the Trp-cage conformation and the subsequent loss of secondary structures. This destabilization is also reflected in the large root mean square deviation (RMSD) of the backbone of TC5b during the course of the 50 ns simulation (Figure 6E).

A cluster analysis was performed based on the backbone RMSD of structures sampled during the course of the simulation. Five thousand structures were grouped into 438 clusters. The middle structure of the largest cluster was sampled at 4600 ps, after the unfolding of the initial structure, most notably the disappearance of the *β*-turn of the central residues. This cluster comprises 309 structures, 6% of the total number of structures. The middle structures of the second largest cluster were sampled at 220 ps, when the Trp-cage was still intact. This cluster comprises 143 structures, about 3% of the total. The middle structure of the third largest cluster was sampled at 30,770 ps, well beyond when the Trp-cage has been unfolded, and comprises 2% of the total. The sheer number of clusters, especially those with less than 10 structures, and the predominance of clusters with average structures divergent from the NMR structures, indicates the

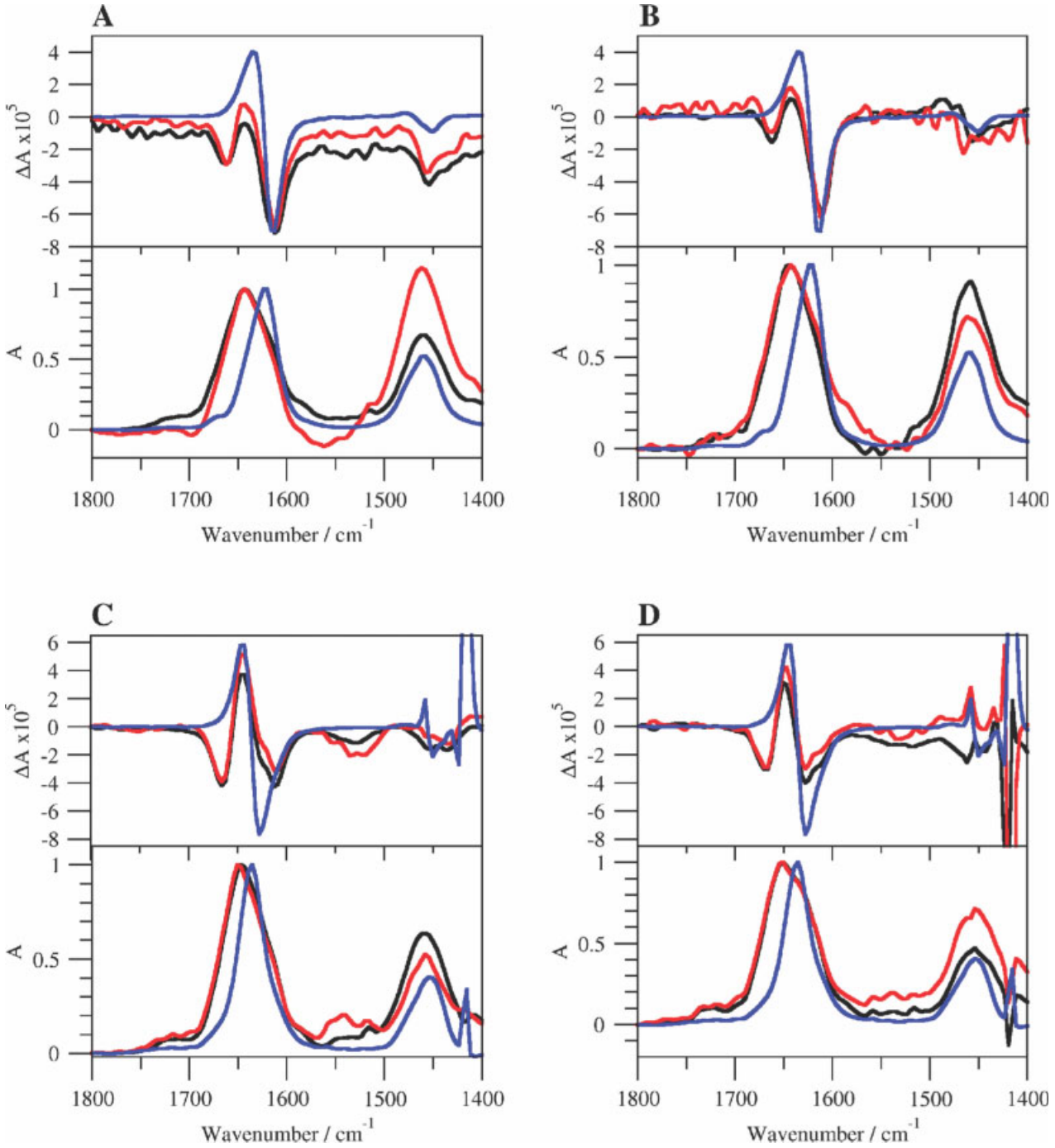

FIGURE 5 Normalized VCD spectra of TC5b and poly-L-Pro in various solvents. Black, TC5b predeuterated; red, TC5b non-predeuterated; blue, poly-L-Pro. (A), D_2O; (B), 15 m*M* Na_2HPO_4 in D_2O; (C), 30% (v/v) TFE-d_1 in 15 m*M* Na_2HPO_4 in D_2O; (D), 5% DMSO-d_6 in TFE-d_1.

strong flexibility and conformational change of TC5b in DMSO.

TC5b structure was also simulated in a 50% (v/v) DMSO in H_2O mixture. DSSP analysis shows that the structure retains some of its α-helix for twice as long as in DMSO (Figure 7A). The β-turn similarly persists in comparison. The Trp6 residue remains near Tyr3, Gly11 (despite moving over 1.5 nm away beginning at 15 ns), Pro12, and Pro18–19 for longer than in pure DMSO, preserving the Trp-cage fold for a few more nanoseconds (Figures 7B and 7C) while the Asp9-Arg16 saltbridge (Figure 7D) follows a similar trajectory to that of the DMSO simulation. The backbone RMSD

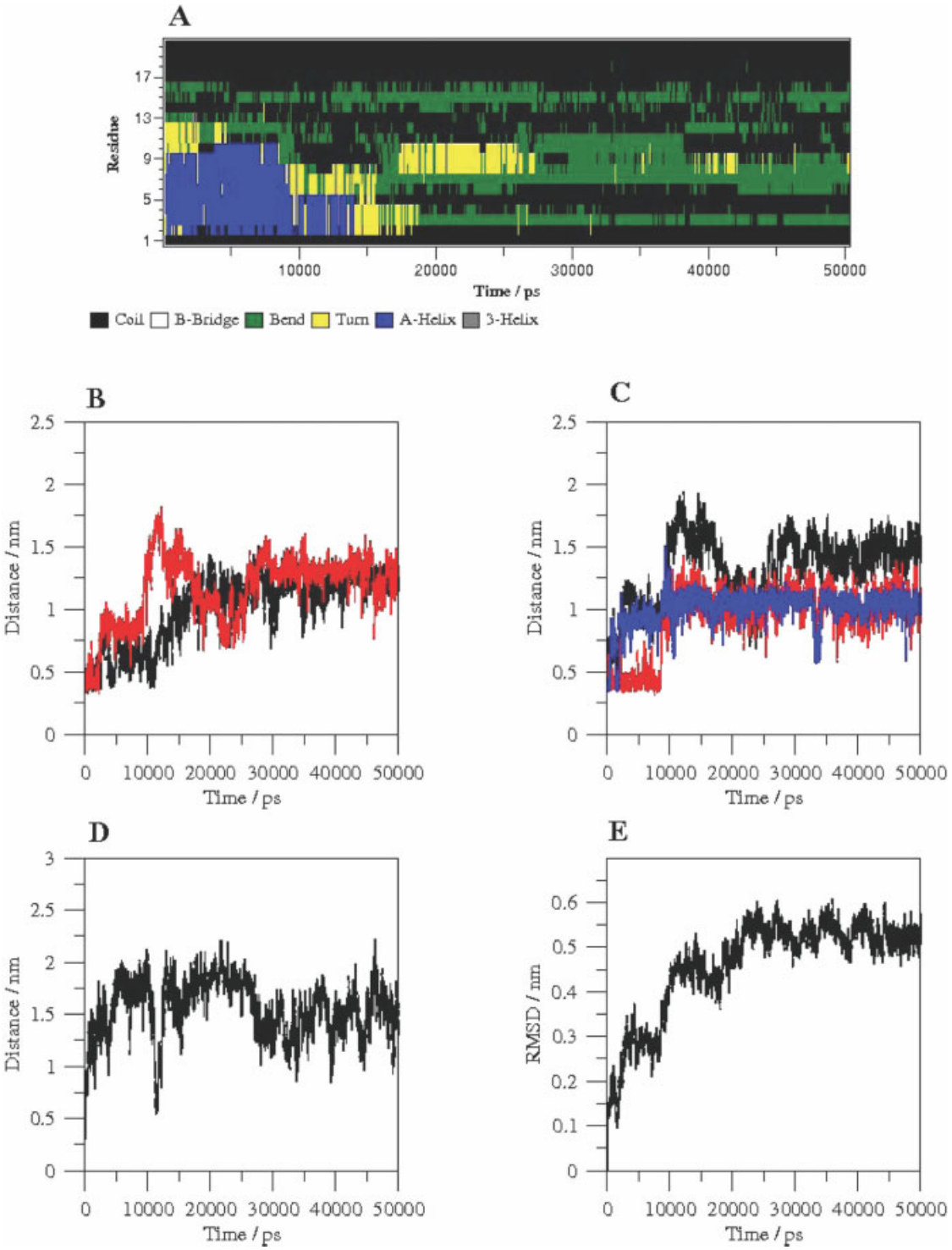

FIGURE 6 MD simulation of TC5b in DMSO. Trajectory analysis: (A) DSSP secondary structure analysis; (B) minimum distance from Trp6 to Tyr3 and Gly11 (black and red, respectively); (C) minimum distance from Trp6 to Pro12, Pro18, and Pro19 (black, red, and blue respectively); (D) saltbridge interaction of Asp9-Arg16; (E) RMSD of the peptide backbone.

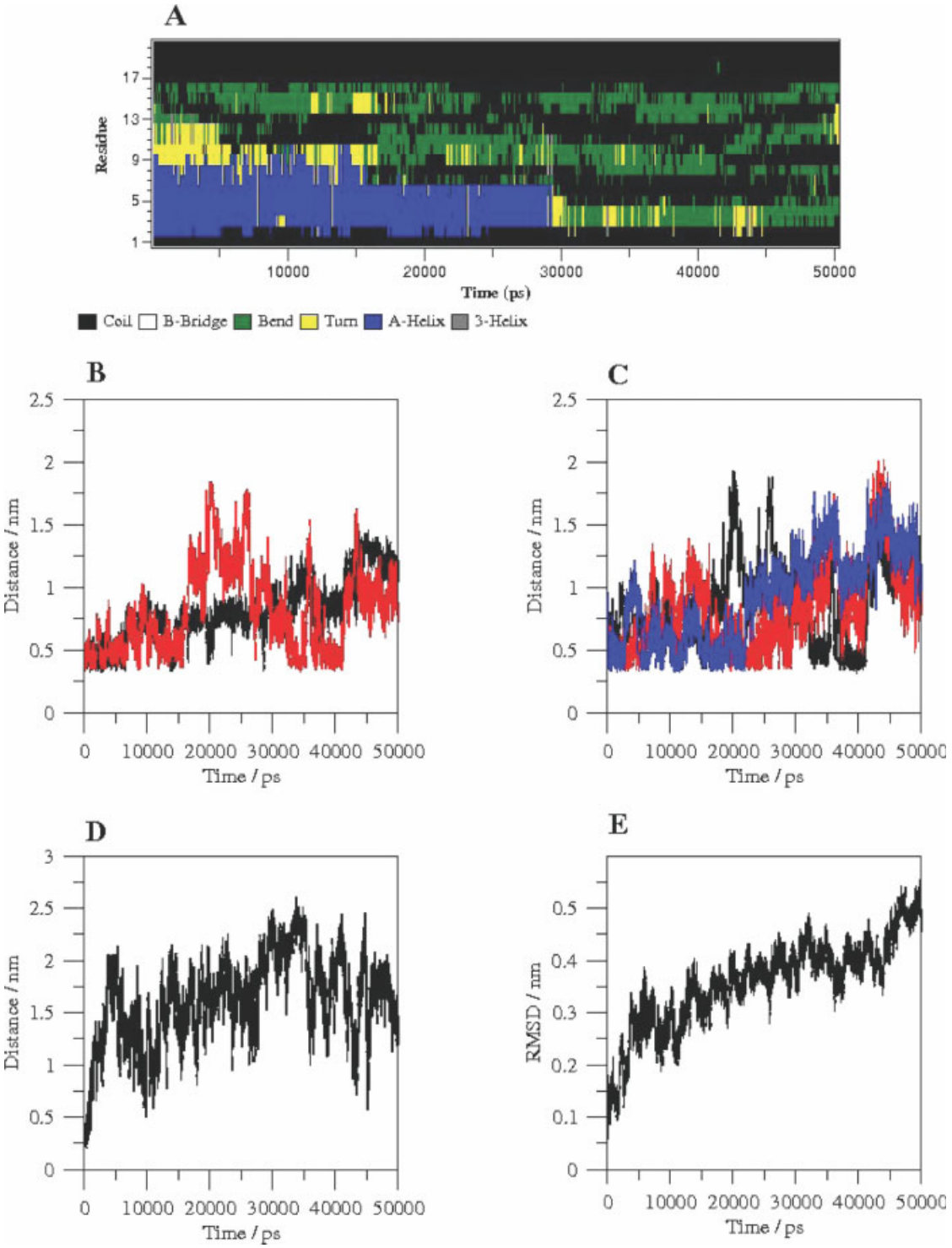

FIGURE 7 MD simulation of TC5b in 50% (v/v) DMSO in H_2O. Trajectory analysis: (A) DSSP secondary structure analysis; (B) minimum distance from Trp6 to Tyr3 and Gly11 (black and red, respectively); (C) minimum distance from Trp6 to Pro12, Pro18, and Pro19 (black, red, and blue, respectively); (D) saltbridge interaction of Asp9-Arg16; (E) RMSD of the peptide backbone.

(Figure 7E) shows a more gradual unfolding of the peptide in the mixture than in DMSO.

A cluster analysis based on the backbone RMSD of structures, sampled during the simulation, grouped 5000 structures into 343 clusters, a smaller number than in pure DMSO. The middle structure of the largest cluster was sampled at 190 ps, when the peptide still retains in the Trp-cage structure. This cluster comprises 211 structures, 4% of the total number of structures. The middle structure of the second largest cluster was sampled at 5310 ps, when some unfolding of the β-turn has occurred, but the initial Trp-cage structure is still largely present. This cluster comprises 152 structures, or about 3% of the total. The middle structure of the third largest cluster was sampled at 8360 ps, when more unfolding of the β-turn has occurred, but the α-helix is still strongly apparent, and comprises about 3% of the total structures. The number of clusters and less-than-10-structures clusters is large, but less than the simulation in DMSO. Additionally, the largest clusters are more comparable in size, and have middle structures more closely resembling the initial NMR structure, indicating less conformational change. Overall, the inclusion of H_2O in the solvent, as expected, mitigates the effect of DMSO on the TC5b structure. Destabilization occurs at a slower rate than in pure DMSO.

These observations are in line with the VCD spectroscopic results, showing the increased flexibility and breakdown of the TC5b α-helical and β-turn structures when the peptide is dissolved in increasing amounts of DMSO. Specifically, the removal of the Gly11, Tyr3, and Pro residues from proximity to the Trp6 residue, disrupting the central Trp-cage structure, is responsible for the loss of secondary structures seen in both the DSSP analysis and the VCD spectra.

CONCLUSION

VCD spectroscopy, while not a replacement for conformational study of peptides with ECD spectroscopy, is a useful tool for qualitatively discerning fine structure that is undetectable with ECD spectroscopy. In this study, VCD spectroscopy has shown explicitly the existence of a PPII helix, where previously only α-helical structure could be seen. Additionally, the determination of VCD spectra of TC5b in various concentrations of DMSO-d_6 in D_2O, an impossibility with ECD, has determined that the peptide loses Trp-cage conformation at greater than 75% DMSO-d_6 in D_2O, and that the structure also disappears at temperatures greater than 35°C. The observation of the PPII helix, together with an α-helix, confirms that the tertiary structure of the synthetic TC5b is similar to that of avian pancreatic polypeptide (aPP); Pro residues from a PPII helix interacting with nonpolar residues of an α-helix to produce a stable fold.[23,24]

Simulation in 50% (v/v) DMSO in H_2O mixture results in the loss of α-helicity in about 28 ns. These data, when combined with the VCD spectra of TC5b in various concentrations of DMSO-d_6 in D_2O, demonstrate the ability of DMSO to solvate TC5b backbone amide groups, unwinding α-helical structure and ultimately reducing its Trp-cage conformation to a series of bends and random meander structures.

EXPERIMENTAL SECTION

Poly-L-Pro (average M_w: 8900 Da) was purchased from Sigma-Aldrich.

TC5b Synthesis and Purification

TC5b was synthesized on an Applied Biosystems 432A Peptide Synthesizer on a Ser-Wang resin (0.025 mmol) using Fmoc protection. For coupling, 3 *M* excess of *N*-α-Fmoc protected amino acids was used. 4-Methyltrityl (Mtt) side chain protection was used for Asn1, as the trityl protection group has been shown to be difficult to cleave in solid phase Fmoc chemistry.[25] In addition, an Asp (*O*-t-butyl (tBu))-Gly (2-hydroxy-4-methoxybenzyl (Hmb)) dipeptide was used in place of Asp9 and Gly10 to prevent aspartimide formation,[26] and Arg16 was double coupled.

The synthesized TC5b was cleaved from the resin by stirring in a 81.5/5/5/5/2.5/1 (v/v/v/v/v/v) TFA/water/thioanisole/phenol/EDT/TIS cleavage mixture for 0.25 h at 0°C, and then for 1.75 h at room temperature. The peptides were precipitated with cold diethyl ether, collected by filtration, dissolved in TFA, and then evaporated to ~1 mL. Peptides were precipitated with cold diethyl ether once again and collected by filtration. Finally, the peptides were dissolved in 10% acetic acid and stirred for 0.5 h to remove the carboxyl group of the *t*-butyloxycarbonyl (Boc) side chain protection group of Trp6. 10% acetic acid was used in the final dissolution of the precipitated peptide to completely remove the aforementioned Boc protection group from Trp6.

Purification was done by reverse-phase high pressure liquid chromatography (RP-HPLC) on a Phenomenex Luna semipreparative or a Vydac preparative C18 column using a dual pump Gilson apparatus. The aqueous phase solvent was water containing 0.1% TFA; the organic phase solvent was acetonitrile containing 0.09% TFA. The purification gradient varied, but generally 25–35% organic phase in aqueous phase for 80 min at a flow rate of 4 or 9 mL/min for semipreparative and preparative columns, respectively, was used. Pure fractions were pooled and lyophilized.

Characterization

Peptides were characterized by RP-HPLC using a Vydac C18 column and the same solvents as used in purification. The gradient was 3–60% organic phase in aqueous phase for 40 min at a flow rate of 1 mL/min. Purified peptides were greater than 95% pure. The correct molecular weight (2169.4 Da) was confirmed by ES-MS using a Perkins Elmer SCIEX API150EX mass spectrometer.

VCD Spectroscopy

VCD spectra were recorded using a BOMEM-Biotools Chiralir Fourier transform VCD spectrometer at 8 cm^{-1} resolution and a 75 mm pathlength CaF_2 cell. In all cases, TC5b (2 mg) was dissolved in either 0.1*M* DCl in D_2O ("predeuterated") or 0.1*M* HCl in H_2O ("non-predeuterated"), lyophilized and then dissolved in 100 mL of deuterated solvent to obtain 20 mg/mL (9.22 m*M*) solutions. No aggregation was observed at this concentration. The solvents tested were: D_2O, 15 m*M* Na_2HPO_4 in D_2O, 30% (v/v) TFE-d_1 in 15 m*M* Na_2HPO_4 in D_2O, 5% (v/v) DMSO-d_6 in TFE-d_1, and DMSO-d_6. Additionally, spectra were recorded in 50% (v/v), 60% (v/v), 70% (v/v), and 75% (v/v) DMSO-d_6 in D_2O. Spectra of DMSO-d_6 measurements were obtained at 25°C; all other single temperature determinations were at 5°C at pH 7. 8 or 12 one-hour-long blocks of spectra were recorded; 4500 scans were performed for VCD and 225 scans were performed for IR absorption in each block. Erroneous blocks were disregarded, and the remainder averaged and corrected for background and water vapor absorption.

For VCD measurements of TC5b structure at increasing temperatures, 2 one-hour-long blocks of spectra were recorded, with the same number of scans as previously. The spectra were averaged and corrected for background and water vapor absorption. Measurements from 15 to 55°C were recorded in 10 degree intervals.

Hour-long measurements of poly-L-Pro spectra in D_2O, 5% (v/v) DMSO-d_6 in TFE-d_1, and DMSO-d_6 were also conducted. In this case, measurements were conducted at a peptide concentration of 15–20 mg/mL (1.69 m*M*–2.25 m*M*) and at a temperature of 5°C. The resultant spectra were corrected for background and water vapor absorption. For comparison to TC5b VCD spectra, poly-L-Pro VCD spectra were divided by 4 (for D_2O and 15 m*M* Na_2HPO_4 in D_2O) or 5 (for 30% (v/v) TFE-d_1 in 15 m*M* Na_2HPO_4 in D_2O and 5% (v/v) DMSO-d_6 in TFE-d_1). To compare the VCD and IR spectra of poly-L-Pro in DMSO-d_6 to measurements of poly-L-Pro in D_2O and 5% (v/v) DMSO-d_6 in TFE-d_1, the VCD spectra of poly-L-Pro in DMSO-d_6 was divided by 4. Poly-L-Pro was difficult to dissolve in DMSO-d_6.

In plotting VCD and IR data for comparison, all spectra were set to zero ΔA and A, respectively, at 1800 cm^{-1}; some points thus may fall below zero in the IR spectra. Additionally, all VCD and IR spectra were normalized by dividing each plot point by the highest peak absorbance in the amide I' region of the IR spectrum, giving an A_{max} of $\sim$1.0 in the amide I' region. The VCD spectrum thus reads directly in $\Delta A/A$ at A_{max}[27].

MD Simulations

MD simulations were performed using TC5b structures obtained from the RCSB Protein Databank (www.rcsb.org) with the GROMACS 3.2.1 package,[28] using the GROMOS 96 force field and the 53a6 parameter set.[29,30] TC5b was solvated in 864 DMSO molecules in the first simulation (100% DMSO), and 2030 H_2O and 398 DMSO molecules in the second simulation (50% (v/v) DMSO in H_2O). A cubic box volume of 125 nm^3 was used in both cases. Structures were energy minimized using the steepest descent method. NVT (constant number of molecules, volume, and temperature) MD simulations were performed with the positionally-restrained peptide for 100 and 1000 ps, respectively, to eliminate differences in solvent density. The resulting structures were used in the MD simulations, which were performed using NPT (constant number of molecules, pressure and temperature) dynamics with periodic box conditions, using constant temperature (300 K) and pressure (1 bar). To avoid the effect of cutoff on long range electrostatic interactions, nonbonded interactions were treated by the twin-range method. 1.2 nm was used for the short range cutoff, 1.6 nm was used for the long range electrostatic cutoff, and 1.5 nm was used for the long range van der Waals cutoff. A reaction-field correction was used for long range electrostatic interactions, and an energy dispersion correction was used for energy and pressure. The simulations were conducted for 50.1 ns each, with an integration step of 2 fs. The first 0.1 ns was considered an equilibration period and subsequently was not used for analysis.

Secondary structures of TC5b generated during the simulations were analyzed using the DSSP method.[31] Trajectories were further analyzed to determine: (1) the minimum distance from the Trp6 to the Tyr3 and Gly11 residues; (2) the minimum distance from the Trp6 to the Pro12 and Pro18-19 residues; (3) the saltbridge length between Asp9 and Arg16; (4) the RMSD of the peptide backbone; (5) the total solvent accessible surface area; (6) the radial distribution function of solvent molecules around the backbone amide hydrogens of TC5b; and (7) the radius of gyration of TC5b. Graphical representations of TC5b were created using the VMD (Visual Molecular Dynamics; www.ks.uiuc.edu/Research/vmd) program. Finally, structures not including the N-terminal Asn residue or the C-terminal Ser residue were sampled at a time step of 10 ps, and grouped into clusters using the algorithm described in Daura et al.,[32] with a cluster RMSD cutoff of 0.1 nm. This was done to examine conformational flexibility of the peptide in each solvent.

REFERENCES

1. Neidigh, J. W.; Fesinmeyer, R. M.; Andersen, N. H. Nat Struct Biol 2002, 9, 425–430.
2. Neidigh, J. W.; Fesinmeyer, R. M.; Prickett, K. S.; Andersen, N. H. Biochemistry 2001, 40, 13188–13200.
3. Toth, G.; Murphy, R. F.; Lovas, S. Protein Eng 2001, 14, 543–547.
4. Qiu, L.; Pabit, S. A.; Roitberg, A. E.; Hagen, S. J. J Am Chem Soc 2002, 124, 12952–12953.
5. Zhou, R. Proc Natl Acad Sci USA 2003, 100, 13280–13285.
6. Neuweiler, H.; Doose, S.; Sauer, M. Proc Natl Acad Sci USA 2005, 102, 16650–16655.
7. Nikiforovich, G. V.; Andersen, N. H.; Fesinmeyer, R. W.; Frieden, C. Proteins 2003, 52, 292–302.
8. Chowdhury, S.; Lee, M. C.; Xiong, G.; Duan, Y. J Mol Biol 2003, 327, 711–717.
9. Snow, C. D.; Zagrovic, B.; Pande, V. S. J Am Chem Soc 2002, 124, 14548–14549.
10. Simmerling, C.; Strockbine, B.; Roitberg, A. E. J Am Chem Soc 2002, 124, 11258–11259.
11. Pitera, J. W.; Swope, W. Proc Natl Acad Sci USA 2003, 100, 7587–7592.
12. Lin, J. C.; Barua, B.; Andersen, N. H. J Am Chem Soc 2004, 126, 13679–13684.
13. Gellman, S. H.; Woolfson, D. N. Nat Struct Biol 2002, 9, 408–410.
14. Polavarapu, P. L.; Zhao, C.; Fresenius, J. Anal Chem 2000, 366, 727–734.
15. Lal, B. B.; Nafie, L. A. Biopolymers 1982, 21, 2161–2183.
16. Borics, A.; Murphy, R. F.; Lovas, S. Biopolymers 2003, 72, 21–24.

17. Seshasayee, A. S. Theor Biol Med Model 2005, 2, 7.
18. Roccatano, D.; Colombo, G.; Fioroni, M.; Mark, A. E. Proc Natl Acad Sci USA 2002, 99, 12179–12184.
19. Kentsis, A.; Sosnick, T. R. Biochemistry 1998, 37, 14613–14622.
20. Hudson, F. M.; Andersen, N. H. Biopolymers 2004, 76, 298–308.
21. Dukor, R. K.; Keiderling, T. A. Biopolymers 1991, 31, 1747–1761.
22. Bochicchio, B.; Tamburro, A. M. Chirality 2002, 14, 782–792.
23. Blundell, T. L.; Pitts, J. E.; Tickle, I. J.; Wood, S. P.; Wu, C.-W. Proc Natl Acad Sci USA 1981, 78, 4175–4179.
24. Copps, J.; Murphy, R.F.; Lovas, S. Biopolymers, 2006, 83, 32–38.
25. Friede, M.; Denery, S.; Neimark, J.; Kieffer, S.; Gausepohl, H.; Briand, J. P. Pept Res 1992, 5, 145–147.
26. Mergler, M.; Dick, F.; Sax, B.; Weiler, P.; Vorherr, T. J Pept Sci 2003, 9, 36–46.
27. Baumruk, V.; Huo, D.; Dukor, R. K.; Keiderling, T. A.; Lelievre, D.; Brack, A. Biopolymers 1994, 34, 1115–1121.
28. Lindahl, E.; Hess, B.; van der Spoel, D. J Mol Model 2001, 7, 306–317.
29. Oostenbrink, C.; Villa, A.; Mark, A. E.; van Gunsteren, W. F. J Comput Chem 2004, 25, 1656–1676.
30. Oostenbrink, C.; Soares, T. A.; van der Vegt, N. F. A.; van Gunsteren, W. F. Eur Biophys J 2005, 34, 273–284.
31. Kabsch, W.; Sander, C. Biopolymers 1983, 22, 2577–2637.
32. Daura, X.; Gademann, K.; Jaun, B.; Seebach, D.; van Gunsteren, W. F.; Mark, A. E. Angew Chem Int Ed Engl 1999, 38, 236–240.